(Received 1 December 2023, Accepted 9 March 2024, Scheduled 29 March 2024)

Recent Advances in Parity-Time Symmetry-Enabled Electromagnetic Sensors

Minye Yang[1,2], Zhilu Ye[1,3], Pai-Yen Chen[1], and Danilo Erricolo[1,*]

[1] *Department of Electrical and Computer Engineering, University of Illinois Chicago, Chicago, IL 60607, USA*
[2] *State Key Laboratory for Manufacturing Systems Engineering, Electronic Materials Research Laboratory, Key Laboratory of the Ministry of Education, School of Electronic Science and Engineering, Xi'an Jiaotong University, Xi'an, Shaanxi 710049, China*
[3] *State Key Laboratory for Manufacturing Systems Engineering, The Key Laboratory of Biomedical Information Engineering of Ministry of Education, Center for Mitochondrial Biology and Medicine, School of Life Science and Technology, International Joint Laboratory for Micro/Nano Manufacturing and Measurement Technology, Xi'an Key Laboratory for Biomedical Testing and High-end Equipment, Xi'an Jiaotong University, Xi'an, Shaanxi 710049, China*

ABSTRACT: Parity-time (PT) reversal symmetry, as a representative example in the field of non-Hermitian physics, has attracted widespread research interest in the past few years due to its extraordinary wave dynamics. PT symmetry enables unique spectral singularities including the exceptional point (EP) degeneracy where two or more eigenvalues and eigenvectors coalesce, as well as the coherent perfect absorber-laser (CPAL) point where laser and its time-reversal counterpart (i.e., coherent perfect absorber) can coexist at the same frequency. These singular points not only give rise to new physical phenomena but also provide new plausibility for building the next-generation sensors and detectors with unprecedented sensitivity. To date, investigations into EPs and CPAL points have unveiled their great potential in various sensing scenarios across a broad spectral range, spanning optics, photonics, electronics, and acoustics. In this review article, we will discuss ongoing developments of EP- and CPAL-based sensors composed of PT-synthetic structures and offer a glimpse into the future research directions in this emerging field.

1. INTRODUCTION

Sensing is a fundamental piece of technology in modern society that has enabled us to perceive and comprehend the intricacies of the world through the measurement of physical, chemical, or physiological quantities such as motions [1–3], vital signs, and concentration of gas, molecules, and ions [4–8]. Particularly, with the rapid advent of the wireless and lightwave technologies, there has been an explosive proliferation of connected smart devices, fostering a rich landscape of information exchange among humans, devices, and intelligent terminals [9, 10] imposing an unprecedented demand for sensors and sensor networks [11, 12]. Wireless sensors have shown their importance in a wide range of applications where wired connection is difficult or impossible; examples include healthcare diagnostics [1–15], environmental monitoring [16–18], intelligent vehicles [19, 20], and food quality control (smart packaging) [21, 22] that leverage the variation of different physical and/or chemical signals. When considering scenarios like nano-crack sensing [23, 24], nondestructive evaluation for civil infrastructures [25, 26], and single-nanoparticle sensing [27], the need for sensors capable of detecting subtle perturbations becomes even more critical.

Conventional electromagnetic sensing technologies are mainly based on the Hermitian degeneracy-diabolic point (DP) [28, 29]. At the DP, only eigenvalues will degenerate, while the corresponding eigenvectors remain orthogonal. Perturbations can lead to a linear shift in the resonance frequency and variation in the resonance line shape. Typically, the resonance frequency shift ($\Delta\omega$) around a DP scales linearly with the strength of the perturbation (ε): $\Delta\omega \propto \varepsilon$. This linear scaling poses a challenge when dealing with extremely small perturbations, as the shift may not be distinguished, especially when the system exhibits a low-Q resonance. In this regard, researchers have extended the investigations from Hermitian to non-Hermitian systems in pursuit of higher sensitivity.

Non-Hermitian physics [30], a century after the birth of quantum mechanics, has revolutionized our understanding that real eigenvalues can be found even in a non-Hermitian Hamiltonian, which commutes with combined parity ($\mathcal{P}$) and time-reversal ($\mathcal{T}$) operators, so-called PT symmetry [31–35]. PT-symmetry was first proposed by Bender and Boettcher in 1998 [36]. A few years later, the notion of PT symmetry was extended to more generalized non-Hermitian Hamiltonians [37], followed by the investigation of the spectral singularities arising from PT symmetry. There are two main types of singularities: exceptional point (EP) and coherent perfect absorber-laser (CPAL) point. The former singularity can be classified as a unique spectral degeneracy that divides the PT-symmetric system into broken and exact PT symmetry phases, for which the eigenvalues of Hamiltonian evolve from complex conjugate pairs in the broken phase to real numbers in the exact phase, with eigenvalues coalescing at the

* Corresponding author: Danilo Erricolo (derric1@uic.edu).

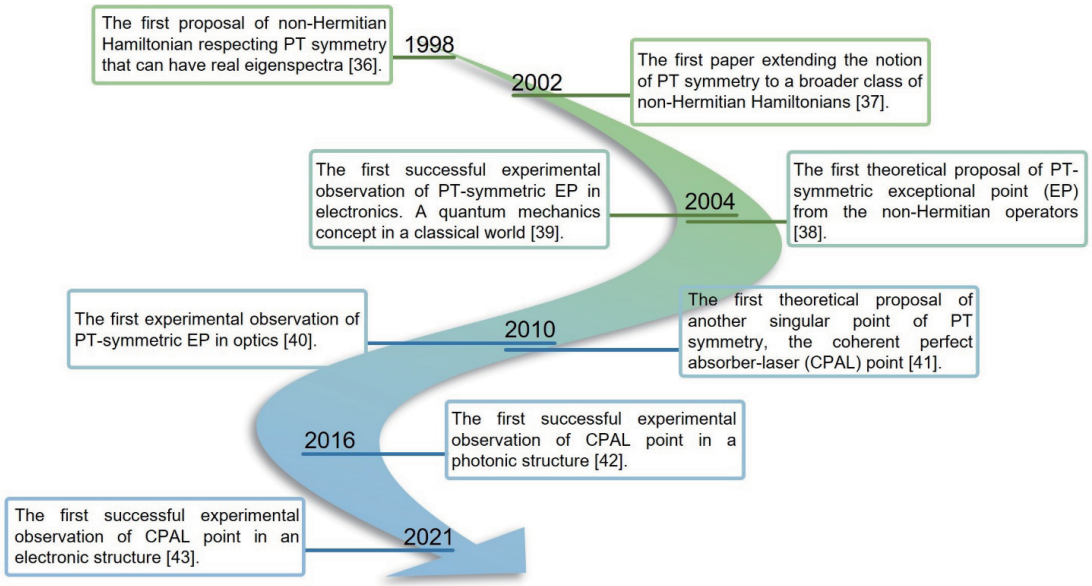

FIGURE 1. Chronological overview of key milestones in the evolution of parity-time (PT) symmetry and its spectral singularities.

transition point-EP [44–47]. Unlike a DP, both eigenvalues and eigenvectors coalesce at an EP. The EP-singularity has given rise to many applications, including unidirectional reflectionless propagation [48–50], non-reciprocity [51–59], single-mode lasing [60], high-performance encryption [61, 62], and robust wireless power transfer [63–68], to name a few. In addition to the EP, another self-dual singularity arises in the broken PT symmetry phase, where the two eigenvalues of the system's scattering matrix become zero and infinity at the same frequency which respectively stand for the coherent perfect absorption (CPA) and lasing [69–71], the so-called CPAL point [41]. CPA is generally regarded as the time-reversed counterpart of lasing [72], so in a common sense they cannot coexist in the same structure at the same frequency. However, PT-symmetric physical systems can make these two opposite phenomena coexist [73], leading to several new applications such as low-threshold lasing [74], superdirective antennas and artificial medium with extreme refractive index [75, 76], and high-contrast optical switching [42]. Fig. 1 illustrates some important milestones of exotic physics associated with EP and CPAL singularities in the PT-symmetric physical systems [38–43].

While non-Hermitian and PT-symmetric structures have been widely studied in control and manipulation of waves [77–79], the pronounced sensitivity under perturbations near EP and CPAL singularities have also been proposed to realize ultrasensitive sensors beyond traditional DP-based sensors [80], which will be discussed in detail in this review article. This paper is structured as below. First, we will briefly discuss working principles and applications of EP-based optical, electronic, and acoustic sensors. Then, we will elucidate the CPAL-based monochromatic sensing technique and its practical realization. Finally, we will provide an outlook on the state-of-the-art PT sensors and some future research directions.

2. EXCEPTIONAL POINT-BASED SENSORS

2.1. Principle of EP-Based Sensing

Let us first consider a PT-symmetric optical system consisting of a pair of optical resonators with gain $(-ig/2)$ and loss $(ig/2)$, and an energy coupling rate (κ) between them, as shown in Fig. 2(a) [81]; throughout this review paper, we adopt the time-convention $\exp(i\omega t)$. One can write the dynamics of this structure using the couple-mode theory (CMT) [82]

$$i\frac{\partial}{\partial t}\begin{pmatrix} a(t) \\ b(t) \end{pmatrix} = \begin{pmatrix} \omega_1 - ig/2 & \kappa \\ \kappa & \omega_2 + ig/2 \end{pmatrix}\begin{pmatrix} a(t) \\ b(t) \end{pmatrix} = H\begin{pmatrix} a(t) \\ b(t) \end{pmatrix}, \quad (1)$$

where $\psi(t) = (a(t), b(t))^T$, $a(t)$ and $b(t)$ stand for the amplitude of eigenmodes; H denotes the effective Hamiltonian of the system; and ω_1 and ω_2 are the resonance frequencies of two resonators. With an averaged uncoupled resonance frequency defined by $\omega_0 = (\omega_1 + \omega_2)/2$ and a frequency detuning $\delta = |\omega_1 - \omega_2|/2$, the eigenfrequencies can be obtained as

$$\omega_\pm = \omega_0 \pm \frac{1}{2}\sqrt{4\kappa^2 - (g + 2i\delta)^2}. \quad (2)$$

When $g < 2\kappa$ and $\delta = 0$ (i.e., negligible frequency detuning), the eigenfrequencies are purely real and unimodular, corresponding to the exact PT-symmetric phase. When $g > 2\kappa$, the eigenfrequencies become a complex conjugate pair, corresponding to the broken PT-symmetric phase. In this regard, the transition point between two phases $g = 2\kappa$ is the EP (highlighted in Fig. 2(b)), at which the Taylor series expansion becomes singular and fails to converge, owning to the bifurcation effect. In the proximity of the EP, if a small perturbation occurs

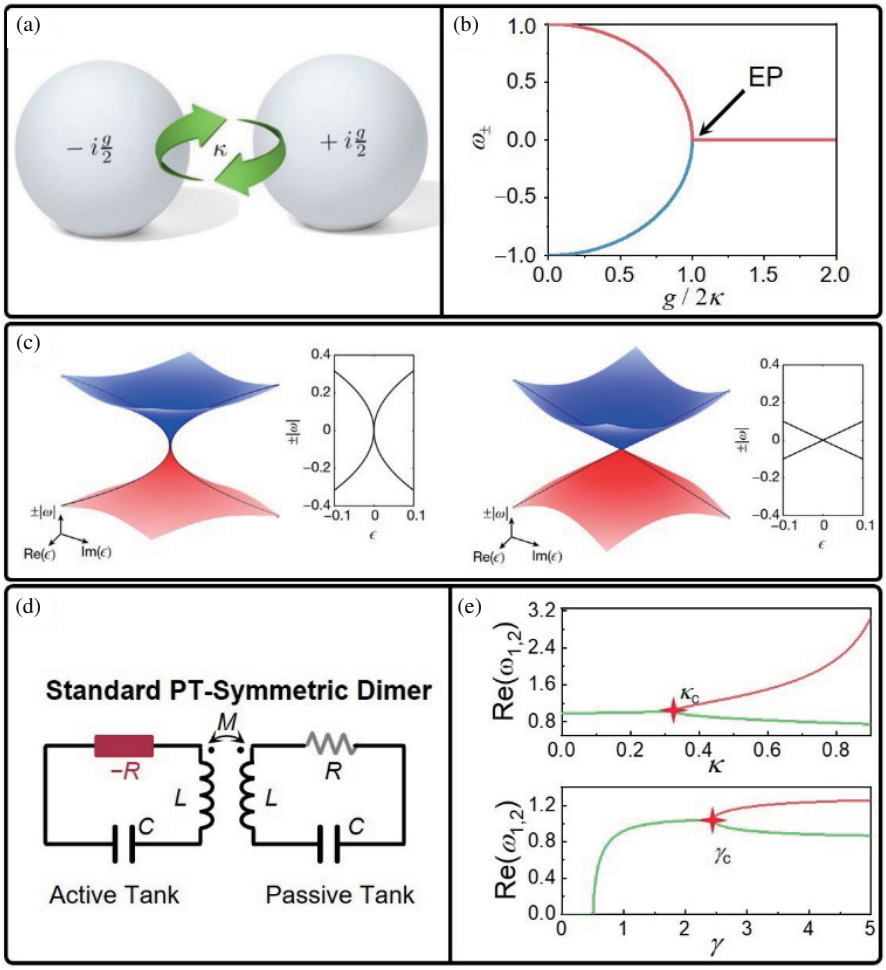

FIGURE 2. (a) Schematic of a PT-symmetric optical system based on coupled optical resonators doped with gain and loss. The energy difference and coupling rate between the two resonators are g and κ. (b) Evolution of eigenfrequencies as a function of the ratio of energy difference to coupling rate; the exceptional point (EP) is observed at $g = 2\kappa$. (c) Contours of the eigenfrequencies as a function of real and imaginary parts of perturbations for an EP sensor (left panel) and a DP sensor (right panel). (d) Schematic of a PT-symmetric electronic circuit consisting of an active $-RLC$ oscillator and a passive RLC oscillator (e) Eigenfrequencies of the electronic PT system in (d) as a function of the non-Hermiticity γ (top panel) or the coupling strength κ (bottom panel). (c) is reprinted with permission from Ref. [83]. Copyright ©2017, Springer Nature; (d) and (e) are reprinted with permission from Ref. [87]. Copyright ©2022, IEEE.

on the gain side (i.e., $\varepsilon \ll 1$), the eigenfrequencies splitting is given by $\Delta\omega = \sqrt{\varepsilon(g+\varepsilon)} \approx (g\varepsilon)^{1/2}$. This property can be exploited to build ultrasensitive optical sensors that can exhibit enhanced sensitivity under small perturbations compared to DP-based sensors [see Fig. 2(c)] [83].

In PT-symmetric electronics, resonators with spatially-distributed, balanced gain and loss can be readily realized using an active-RLC oscillator and a passive RLC oscillator, which are contactlessly coupled via a mutual inductance, mutual capacitance, or both, as shown in Fig. 2(d). In PT-symmetric electronics, applying the Kirchhoff's law to the circuit in Fig. 2(d) leads to the following results [84, 85]

$$\begin{aligned} \frac{d^2Q_1}{d\tau^2} + \kappa\frac{d^2Q_2}{d\tau^2} - \frac{1}{\gamma}\frac{dQ_1}{d\tau} + Q_1 = 0, \\ \frac{d^2Q_2}{d\tau^2} + \kappa\frac{d^2Q_1}{d\tau^2} + \frac{1}{\gamma}\frac{dQ_2}{d\tau} + Q_2 = 0, \end{aligned} \tag{3}$$

where Q denotes the charges stored in the capacitors; subscripts 1 and 2 represent the active and passive oscillator, respectively; $\tau = \omega_0 t$; the resonance frequency of two oscillators $\omega_0 = 1/(LC)^{1/2}$; the non-Hermiticity (or gain-loss parameter) $\gamma = R^{-1}(L/C)^{1/2}$; the coupling strength $\kappa = M/L$ where $M(L)$ is the mutual (self) inductance. The results in Eq. (3) can be casted into Liouvillian formalism, with an effective non-Hermitian Hamiltonian given by

$$H_{\text{eff}} = i\begin{pmatrix} 0 & 0 & 1 & 0 \\ 0 & 0 & 0 & 1 \\ \frac{-1}{1-\kappa^2} & \frac{\kappa}{1-\kappa^2} & \frac{1}{\gamma(1-\kappa^2)} & \frac{\kappa}{\gamma(1-\kappa^2)} \\ \frac{\kappa}{1-\kappa^2} & \frac{-1}{1-\kappa^2} & \frac{-\kappa}{\gamma(1-\kappa^2)} & \frac{-1}{\gamma(1-\kappa^2)} \end{pmatrix}, \tag{4}$$

from which the eigenfrequencies can be derived as

$$\omega_{1,2} = \omega_0\sqrt{\frac{2\gamma^2 - 1 \pm \sqrt{1-4\gamma^2+4\gamma^4\kappa^2}}{2\gamma^2(1-\kappa^2)}}. \tag{5}$$

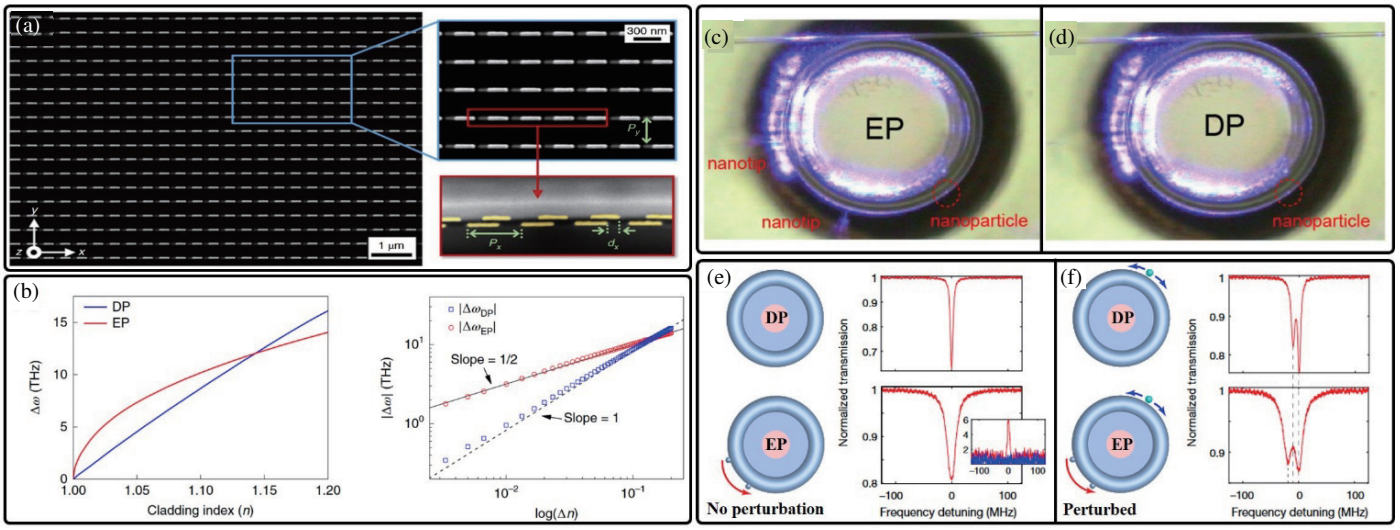

FIGURE 3. (a) Scanning electron microscope image of the EP-based plasmonic sensor. The top view and side view are shown in the right panel. (b) Measured frequency detuning for the EP and DP configurations when perturbed by a thin dielectric coating. (c) and (d) are the optical microscope image of the EP- and DP-based optical microcavity sensor (e) and (f) correspond to their normalized transmission spectra of before and after the nanoparticle-induced perturbation is applied. (a) and (b) are reprinted with permission from Ref. [88]. Copyright ©2020, Springer Nature; (c) and (e) are reprinted with permission from Ref. [83]. Copyright ©2017, Springer Nature.

The Hamiltonian in Eq. (4), although non-Hermitian, can commute with the combined $\mathcal{PT}$ transformation, i.e., $[\mathcal{PT}, H] = 0$ [86]. When the non-Hermiticity and coupling strength exceed certain critical values, the eigenfrequency bifurcation effect can be obtained, as can be seen in Fig. 2(e). Therefore, when a resistive or reactive perturbation $\varepsilon \ll 1$ is introduced to the electronic PT dimer operating at the EP, high sensitivity in terms of resonance frequency shift (which is boosted by eigenfrequency splitting) can be attained.

2.2. EP-Based Optical Sensors

The mathematical structural similarity between Maxwellian and Schrödinger systems makes optical and photonic systems a fruitful playground for experimental studies of non-Hermitian physics, PT symmetry, and EPs. A representative example is the two-layer plasmonic resonant structure shown in Fig. 3(a) [88], where two dissimilar layers of plasmonic resonators are separated by a polymer spacer with one layer exposed to the air such that it can be functionalized for sensing applications. If the same plasmonic structure is used in both layers, the system exhibits a DP, rather than an EP. The system can be readily reconfigured to exhibit an EP by breaking the geometric symmetry through proper misalignment between two layers [see the inset of Fig. 3(a)]. In order to study the sensing performance, a thin dielectric layer that introduces perturbation ε is deposited on the top layer. The authors have tested both EP and DP-based plasmonic structures, and observed that a resonance frequency shift $\Delta\omega \propto \varepsilon^{1/2}$ is obtained in the EP configuration, while a linear change $\Delta\omega \propto \varepsilon$ is obtained in its DP counterpart. Therefore, under small perturbations EP-based sensors can outperform DP-based sensors, as can be seen in Fig. 3(b). Chen et al. compared the performance of EP- and DP-based optical sensors formed by a micro-toroid cavity with parasitic Rayleigh scatterers (silica nano-tips) [83] as shown in Fig. 3(c). When two Rayleigh scatterers are removed, the optical cavity is reconfigured to a DP structure [see Figs. 3(d) and 3(e)], which allows the authors to compare the sensing performance of DP and EP structures. In this case, perturbation is introduced by a silica nano-tip placed in the vicinity of the microtoroid cavity [see Fig. 3(f)]. From the measured transmission spectrum shown in Figs. 3(e) and 3(f), it is evident that the EP-based optical sensor shows a greater frequency detuning, and once again, the shift of transmission dips verifies the theoretical result that EP (DP) configuration follows the square-root (linear) scaling rule under small perturbations.

In [90], Lai et al. have demonstrated that an optical gyroscope [see Fig. 4(a)] operating near an EP can have an enhanced sensitivity in detecting the rotation and Sagnac effect. To satisfy the EP condition, two pump waves with frequency detuning $\Delta\omega_p$ are fed into a microresonator inducing two stimulated Brillouin laser (SBL) in counter-propagation directions. The EP is obtained when $\Delta\omega_p$ is at the critical value $\Delta\omega_c$ where the measured SBL beating angular frequency undergoes a bifurcating effect. When compared with the Sagnac value obtained in conventional optical gyroscope (i.e., $2\pi D/(n_g\lambda)$ where D is the diameter of the microresonator, n_g the group index of the passive cavity mode, and λ the SBL wavelength [91]), the EP-enhanced optical gyroscope can have a boost factor of $\Delta\omega_p/\sqrt{\Delta\omega_p^2 - \Delta\omega_c^2}$, which can substantially increase the Sagnac factor when $\Delta\omega_p$ is mall. Recently, the optical system composed of multiple gain-loss pairs has been proposed to achieve a higher-order EP, which can further amplify the bifurcation effect, as $\Delta\omega \propto \varepsilon^{1/N}$, where N is the order. As reported in [92], a system consisting of four racetrack microring resonators [see Fig. 4(b)] can be tuned to exhibit a fourth-order EP. The relationship between wavelength splitting and cladding

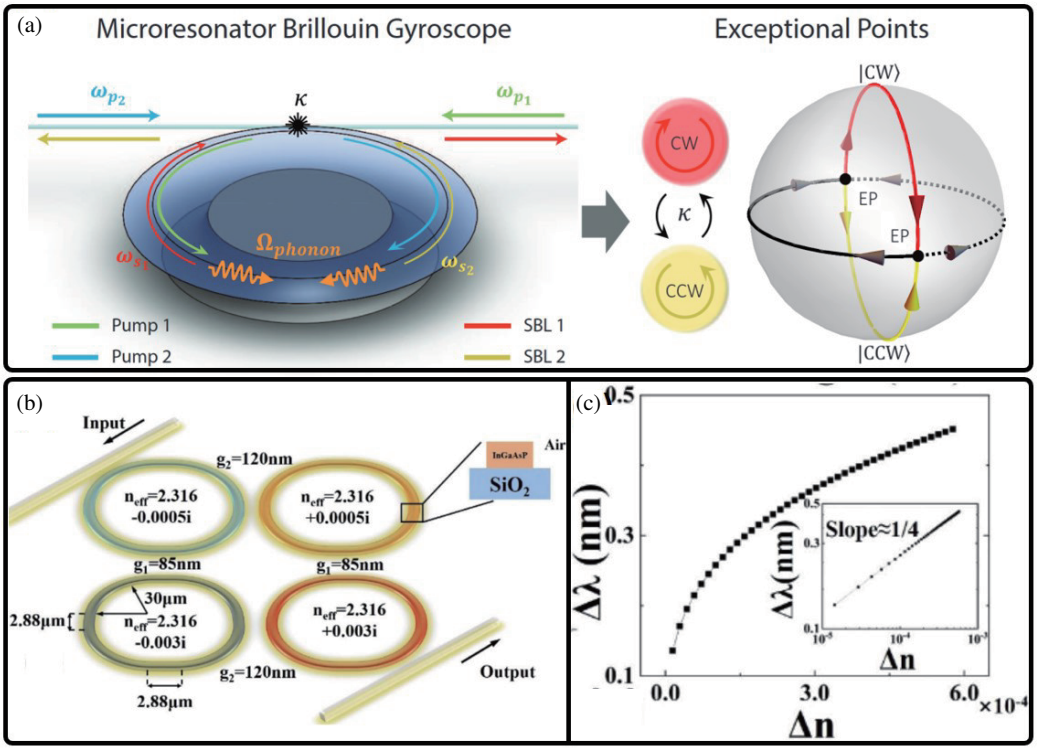

FIGURE 4. Schematics of (a) the EP-based optical gyroscope, and (b) higher-order EP-based optical sensor based on multiple racetrack microring resonators. (c) Measured wavelength splitting against refractive index change for the higher-order EP-based sensor in (b). (a) is reprinted with permission from Ref. [90]. Copyright ©2019, Springer Nature.

refractive index change exhibits a slope of 1/4 on the logarithmic scale, as shown in Fig. 4(c). Such results are in good agreement with the above theoretical predictions and further verify that higher order EP may imply higher sensitivity.

Despite the great potential of EP-based optical and photonic sensors, there are still concerns about using an EP for sensing applications, since their spectral degeneracy may also amplify unwanted flicker noise at the same level. Indeed, high entropy and uncertainty around an EP singularity may pose challenges in practically achieving high signal-to-noise ratio. In [93], Langbein claimed that the achievable sensitivity would be questioned due to the inevitable presence of time-fluctuating noise from the environment during the experiment [81]. In [94] Chen et al. reached a similar conclusion using the quantum Fisher information theory. In [95], Duggan et al. provided a complete study for passive and active optical EP sensors. To mitigate the influence of noise, two approaches may be considered. The first utilizes feedback loops to fine tune system parameters based on noise, forcing the system to operate precisely at an EP [83, 96]. The other approach requires changing the sensing mechanisms in non-Hermitian structures, such as monochromatic CPAL-based sensors discussed in the next section. The first solution may increase the cost and complexity of implementation, whereas the second approach may require precise and coherent control of the amplitude and phase of two incident waves. The practical use and deployment of EP-based optical sensors still requires more investigations, especially in noise analysis and suppression.

2.3. EP-Based Electronic and Acoustic Sensors

Beyond the exploration of EP sensors in the optical domain, their realizations in electronics and acoustics have also emerged in the past decade. A representative example of the electronic EP sensor was demonstrated in 2018 [86] and illustrated in Fig. 5(a). In this work, the generalized PT-symmetric electronic circuit was built using the inductively coupled gain and loss, which in the realm of electronics are composed of an active −RLC oscillator (reader) and a passive RLC oscillator (microsensor), respectively, as can be seen in Fig. 5(a). When a pressure-induced capacitive perturbation arises in the sensor (RLC oscillator), the resonance frequency shift can sensitively respond to it, in light of bifurcating eigenfrequencies near an EP. This is in sharp contrast to conventional telemetric sensing systems using a passive coil antenna to interrogate the same sensor, as can be seen in Fig. 5(b). Moreover, the generalized PT-symmetric electronic system with additional reciprocally scaling symmetry can relax constraint on the gain-loss balance. Noticeably, the generalized PT-symmetry and standard PT symmetry share the same eigenspectrum but different eigenstates, allowing tailoring the resonance lineshape/linewidth and Q-factor that affect the sensing resolution. This pioneering work opens up a new avenue for wireless sensing solutions, addressing the longstanding challenges of wireless readout of passive micro/nanosensors.

Later on, the 6^{th}-order EP-based electronic sensor [see Fig. 6(a)] was proposed to further increase the sensitivity of the electronic EP sensors and suppress the effect of noise [97]. In

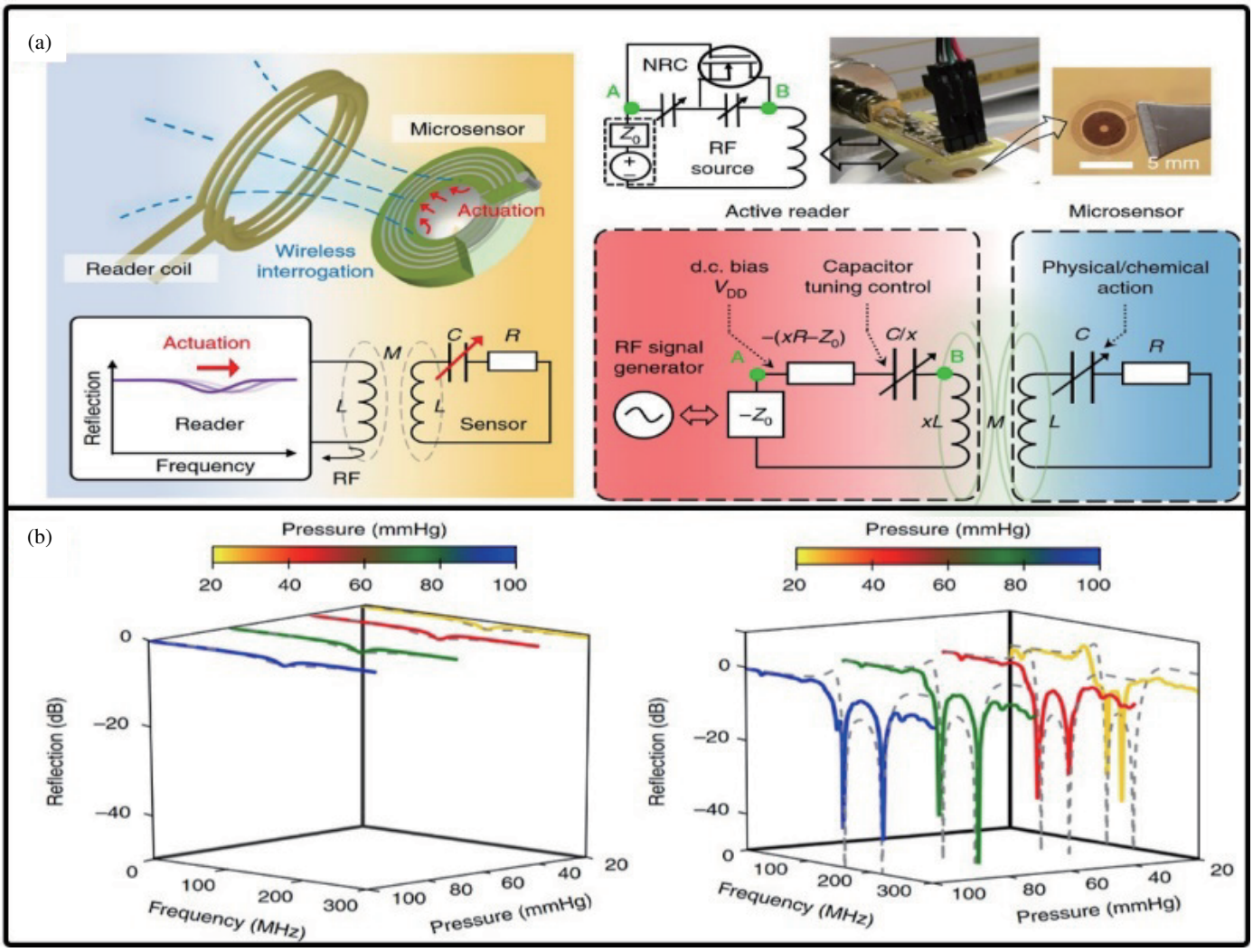

FIGURE 5. (a) Diagram of the traditional (left panel) and the EP-based PT-symmetric (right panel) telemetric sensing system (b) Evolution of frequency detuning under perturbations, measured by the traditional (left panel) and EP-based (right panel) telemetric sensing systems. (a) and (b) are reprinted with permission from Ref. [86]. Copyright ©2018, Springer Nature.

this higher-order PT electronic system, the resonance frequency splitting follows $\Delta\omega \propto \varepsilon^{1/4}$. Therefore, when the mutual capacitance is disturbed by, for example, microfluid, pressure, and acceleration-sensitive capacitor, the resonance frequency shift can be dramatic. Notably, this work compares sensitivity with that of the DP-based electronic sensor to manifest the enhancement brought by the EP-based structure. This work also studies the noise figure of the EP-based electronic sensor and shows that the noise figure is very small in higher-order PT electronic systems, with a noise power spectrum density close to zero. In this context, recently, a similar EP-based accelerometer utilizing transmission peak degeneracy (TPD) [see Fig. 6(b)] was proposed to suppress the excess noise sourced from the eigenbasis collapse and amplification of devices' noise at an EP [98, 99]. In this design, two shunt "$-$RLC" and "RLC" oscillators are capacitively coupled, and one terminal of the coupling capacitor is connected to the test mass; two capacitors C_e are used to couple signals to a transmission line for data acquisition. Different from those EP-based sensors relying on the frequency detuning, this accelerometer measures the difference between EP and TPD via a weakly coupled transmission line. This EP-based accelerometer can achieve the desired sensitivity as typical EP-based sensors, while conserving the complete eigenbasis to avoid the noise due to the eigenbasis collapse. The measurement results show a three-fold reduction in the noise enhancement factor, effectively mitigating the amplification of naturally existing technical noise such as thermal and flicker noise.

EP-based acoustic sensors have also sparked considerable interest [100–103]. In [104], an invisible EP-based acoustic sensor is presented [see Fig. 6(c)]. The system comprises an active and a passive loudspeaker separated by an acoustic transmission line. Here, we must stress that in contrast with the conventional EP sensors monitoring the splitting of the eigenfrequencies, this acoustic EP sensor makes use of the power absorbed by the passive loudspeaker as the sensing principle.

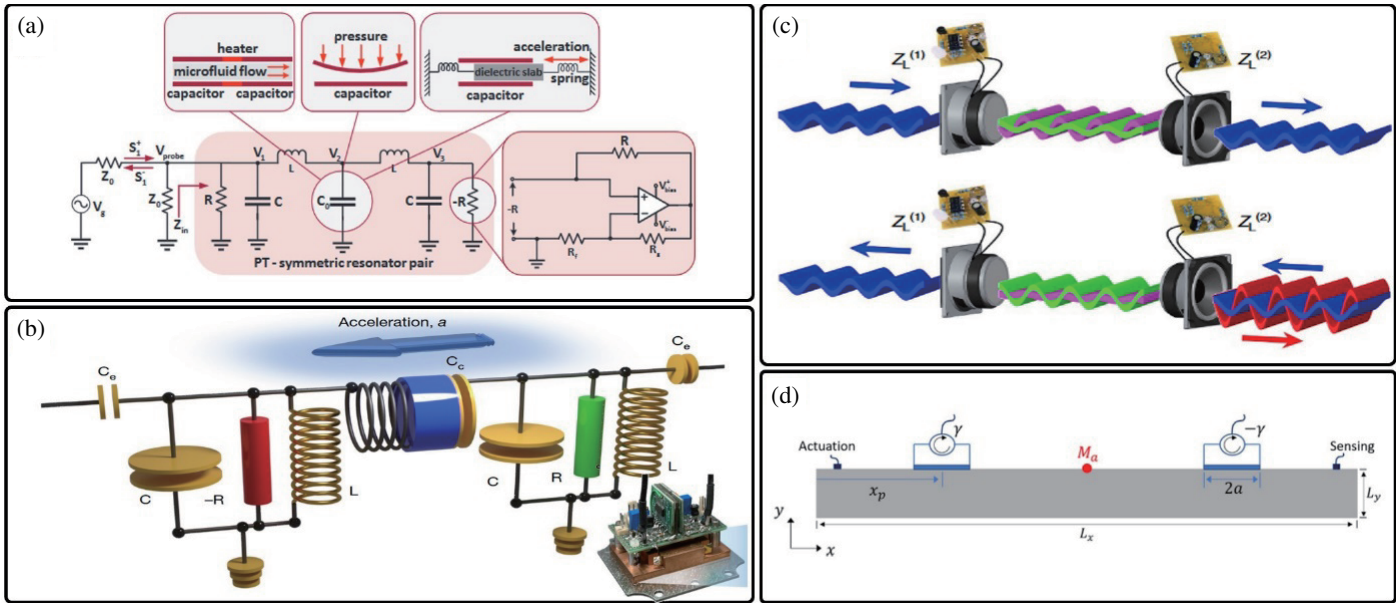

FIGURE 6. (a) Schematic of the 6th-order EP-based electronic sensor. The coupling capacitor can be replaced by a microfluid-, pressure-, or acceleration-sensitive capacitor. (b) The circuit diagram and prototype of an EP-based accelerometer utilizing the transmission peak degeneracy (TPD) principle. (c) Invisible acoustic sensor operating at an EP, of which PT-symmetric acoustic system is formed by an active loudspeaker and a passive loudspeaker, which are separated by a transmission line. (d) EP-based elastic sensor formed by elastic media loaded with two springs of complex spring constant. (a) is reprinted with permission from Ref. [97]. Copyright ©2019, American Physical Society; (b) is reprinted with permission from Ref. [99]. Copyright ©2022, Springer Nature; (c) is reprinted with permission from Ref. [104]. Copyright ©2015, Springer Nature; (d) is reprinted with permission from Ref. [107] Copyright ©2021, Elsevier.

At the EP found in the eigenvalues of the scattering matrix, anisotropic transmission resonance (ATR) [105] can be observed where reflections at the two ports are zero and unitary, respectively. The scattering matrix (S) of the PT acoustic system shown in Fig. 6(c) can be written as: $S = \begin{pmatrix} t & r_+ \\ r_- & t \end{pmatrix} = \begin{pmatrix} e^{ix} & 2 - 2e^{2ix} \\ 0 & e^{ix} \end{pmatrix}$, where t and $r_\pm$ are transmission and reflection coefficients on right and left sides, and x is the acoustic length between two loudspeakers. It is obvious that when sound waves are incident from the left, the structure can be invisible (i.e., $r_- = 0$). Furthermore, by sending acoustic waves from the active loudspeaker side, the incident wave may be fully absorbed (sensed) by the passive loudspeaker that acts as an acoustic power sensor. This concept, although proven in the field of acoustics, may also be applied to optical and electronic sensors [106]. Another EP-based elastic sensor utilizing the eigenfrequency splitting is presented in Fig. 6(d) [107]. This sensor comprises two springs with conceptually complex spring constants loaded on two sides of the elastic media. A point mass placed in the middle of the structure introduces perturbation to the system. When the loaded mass increases, the eigenfrequencies of the system undergo the bifurcation process, which, in some sense, is similar to the EP-based electronic and optical sensors. Emerging EP-based sensors in optics [77, 108–111], plasmonics [112], electronics [113–118], and acoustics [119, 120] indeed open up new directions for development of the next-generation electromagnetic sensors. They can be used in a variety of applications, ranging from the detection of nanoparticles to the measurement of macroscopic physical/chemical quantities. Despite several ongoing research on how to eliminate the effects of noise generated near an EP, EP-based sensors may see a bright future as technological advancements in device fabrication and measurement instruments are expected to effectively address the noise issues.

3. COHERENT PERFECT ABSORBER-LASER-ENABLED SENSING

Back in 2010, Longhi mathematically demonstrated that PT-symmetry enables lasing and its time-reversed counterpart CPA to coexist within a single optical cavity, so-called CPAL phenomenon [41]. Consider the PT-symmetric metasurfaces in Fig. 7(a) [121–124], gain and loss separated by a dielectric spacer represented by an active metasurface with surface conductance $G_{\text{gain}} = -\eta Y_0$ and a passive metasurface with $G_{\text{loss}} = \eta Y_0$ where η is the dimensionless gain-loss factor, and Y_0 is the characteristic admittance of free space. This PT optical system can be modeled using an equivalent transmission line network model shown in Fig. 7(b). Assume that there are two light waves impinging from both sides of this cavity as $|\psi_{\text{in}}\rangle = (\psi_{\text{in}}^+, \psi_{\text{in}}^-)^T$, where ψ is the wave amplitude, and $\pm$ denotes light incidents from the top and bottom directions [see Fig. 7(a)]. The incident and outgoing light can be related by the scattering matrix (S) as: $|\psi_{\text{out}}\rangle = S\,|\psi_{\text{in}}\rangle$ where $|\psi_{\text{out}}\rangle = (\psi_{\text{out}}^+, \psi_{\text{out}}^-)^T$.

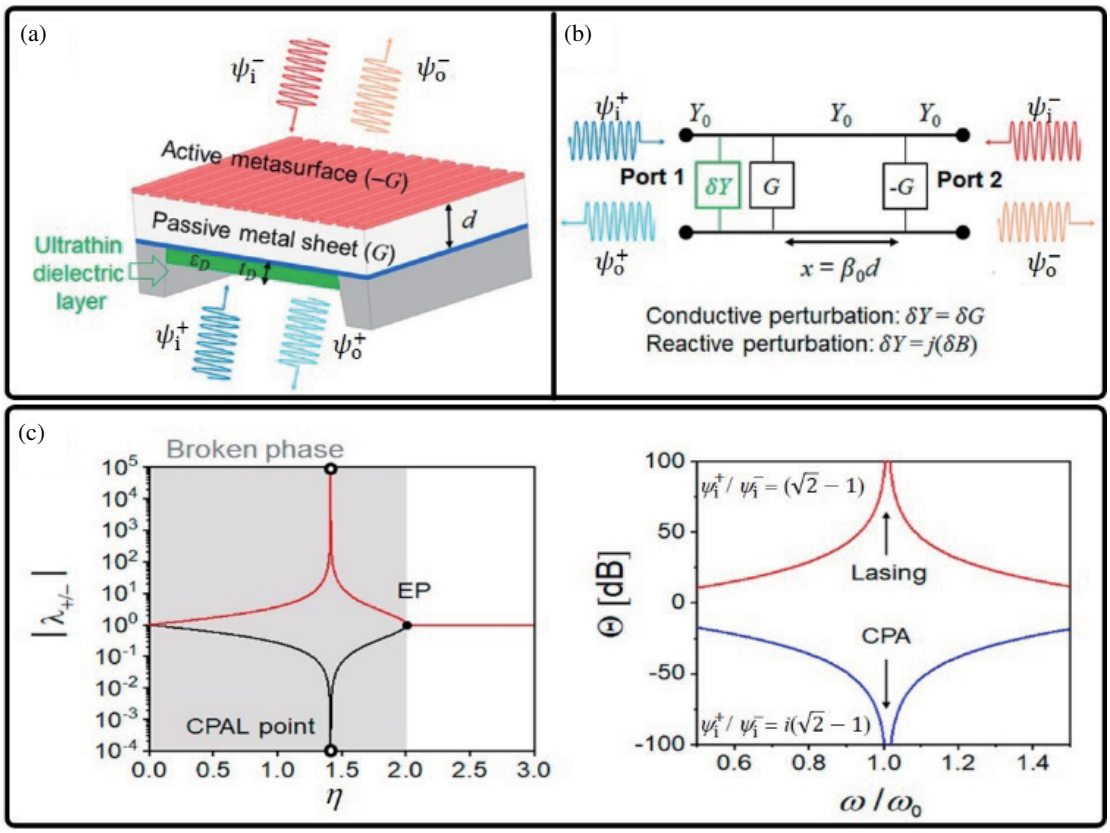

FIGURE 7. (a) Schematic and (b) equivalent transmission line network model of PT-symmetric metasurfaces. (c) Eigenvalues of the scattering matrix as a function of the gain-loss factor (left) and output factor in the lasing mode and the CPA mode (right). (a), (b), and (c) are reprinted with permission from Ref. [122] Copyright ©2020, American Chemical Society.

The scattering matrix simply reads

$$S = \begin{pmatrix} t & r_+ \\ r_- & t \end{pmatrix} = \begin{pmatrix} \frac{2i\csc(x)}{-2+\eta^2+2i\cot(x)} & \frac{-\eta(\eta+2)\sin(x)}{-2+\eta^2+2i\cot(x)} \\ \frac{-\eta(\eta-2)\sin(x)}{-2+\eta^2+2i\cot(x)} & \frac{2i\csc(x)}{-2+\eta^2+2i\cot(x)} \end{pmatrix}, \quad (6)$$

where $r_\pm$ represents the reflection coefficients, t the transmission coefficient, and x the electrical length of the dielectric spacer. One can easily verify that the scattering matrix satisfies the relation $S^*(\omega) = \mathcal{PT}S(\omega)\mathcal{PT} = S^{-1}(\omega)$. The PT phase transition can be observed from the eigenvalues of the scattering matrix. For a quarter-wavelength dielectric spacer (i.e., $x = \pi/2$), the eigenvalues degeneracy is obtained at $\eta_{\text{EP}} = 2$, as shown in Fig. 7(c). The CPAL point ($\eta_{\text{CPAL}} = \sqrt{2}$) can be obtained in the broken PT-symmetric phase, for which one eigenvalue approaches infinity (i.e., lasing mode), while the other eigenvalue is zero (i.e., CPA mode). Of course, it is impossible to achieve an infinite eigenvalue in the experiment, since electronic and optical components with nonlinearities and a limited dynamic range prevent the eigenvalue from becoming infinite. Therefore, in practice, the "lasing" point should be referred to as the "amplification" or "emitter" point. The output factor of the system can be defined as the ratio of the total output power (proportional to $|\psi_{\text{out}}\rangle^2$) to the total input power (proportional to $|\psi_{\text{in}}\rangle^2$): $\Theta = |\psi_{\text{out}}\rangle^2 / |\psi_{\text{in}}\rangle^2$. Ideally, the system locked at the CPAL point has a zero output factor ($\Theta \to 0$) when $\psi_{\text{in}}^+/\psi_{\text{in}}^- = i(\sqrt{2}-1)$, or an infinitely large output factor ($\Theta \to \infty$) when $\psi_{\text{in}}^+/\psi_{\text{in}}^- \neq i(\sqrt{2}-1)$, as shown in Fig. 7(c).

The CPAL point as a self-dual singularity can also be exploited to build ultrasensitive sensors. A CPAL-based metasurface sensor was reported in [122]. As illustrated in Fig. 8(a), the optically-pumped active metasurface with negative surface conductance [125, 126] is paired with a lossy resistive sheet. The CPAL sensor is initially locked at the CPA state with output factor being nearly zero ($\Theta \approx 0$). Upon resistive or reactive perturbation, the operating state of the system can be switched from CPA to lasing, with a drastic modulation in the output factor from near zero to a large value, as shown in Fig. 8(a). The theoretical results show that the CPAL sensor can respond to even low perturbation of only 10^{-6}. Also, this monochromatic sensor can be potentially free of thermal and flicker noise, ensuring a high signal-to-noise ratio (SNR). CPAL sensors based on the generalized PT-symmetric metasurfaces are reported in [127].

The possibility of making a CPAL-based sensor was demonstrated using an electronic circuit simulating the equivalent transmission line model in Fig. 7(b) [43] [see the inset of Fig. 9(a)]. In this CPAL-based electronic sensor, gain and

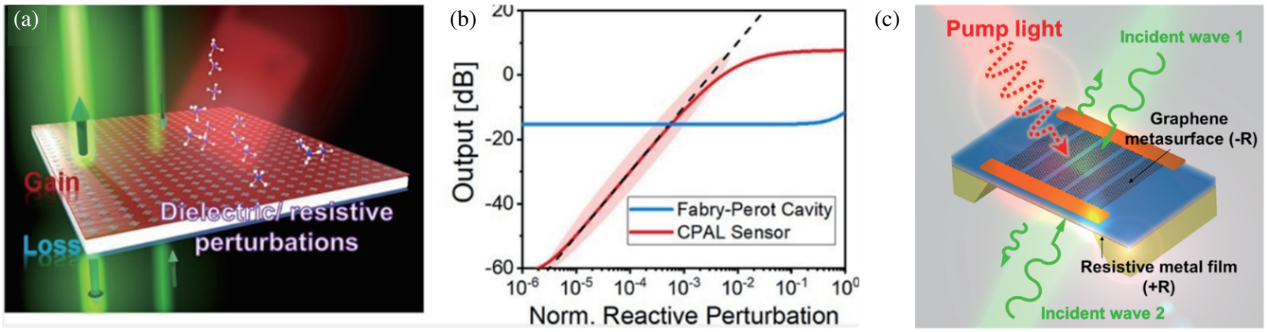

FIGURE 8. (a) CPAL-based optical sensor based on PT-symmetric metasurfaces, and (b) its output factor as a function of normalized perturbations. (c) Practical realization of PT-symmetric metasurfaces using graphene metasurfaces (gain) and resistive metal filament (loss). This figure is reprinted with permission from Ref. [122]. Copyright ©2020, American Chemical Society.

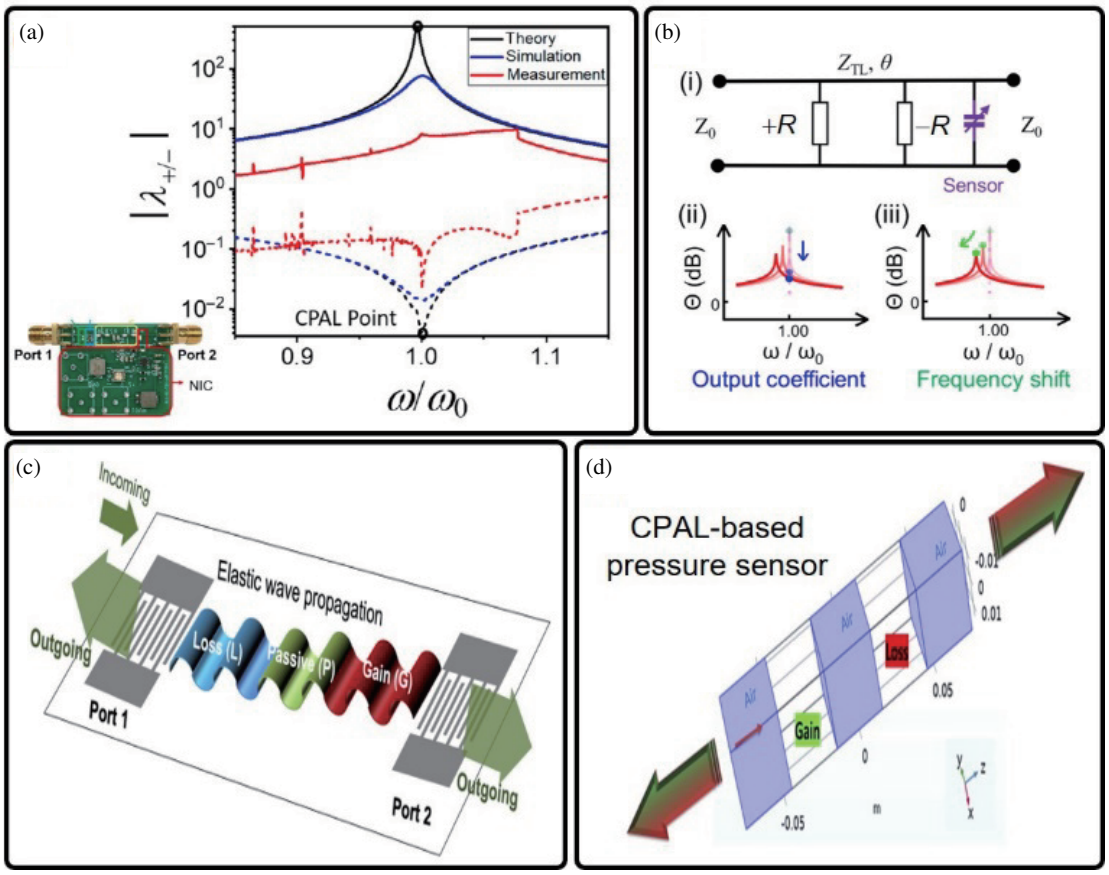

FIGURE 9. (a) Measured and calculated eigenvalues of the scattering matrix of the electronic CPAL sensor with its prototype shown in the inset. (b) Electronic CPAL sensor adopts similar circuit topology in (a), but different sensing mechanism-detecting the shift of CPAL frequency (c) Diagram of an elastic CPAL sensor used for detecting small-scale vibrations. (d) Diagram of an acoustic CPAL sensor used for air pressure sensing. (a) is reprinted with permission from Ref. [43]. Copyright ©2021, American Physical Society; (b) is reprinted from Ref. [129] with permission. Copyright ©2023, AIP Publishing; (c) is reprinted with permission from Ref. [130]. Copyright ©2021, American Physical Society.

loss are given by a negative impedance converter (NIC) and a lumped resistor, respectively, and a T-equivalent transformer can function as a transmission line segment. The measured eigenvalues reported in Fig. 9(a) show that the CPAL-based electronic sensor can detect perturbations at a level of 10^{-3}. On the other hand, a traditional Fabry-Pérot (FP) interferometer-based sensor fails in distinguishing such small perturbations. Due to the nonlinearity of active devices, parasitics of electronic components on the printed circuit board and fabrication errors, the system deviates slightly from the CPAL point, which makes the sensor less sensitive than expected from the theoretical prediction. We note that sensitivity can be further im-

TABLE 1. Summary of EP and CPAL sensors.

Ref.	Type	Frequency/ wavelength	Configuration	Gain realization	Target	Sensitivity	Tunability	Noise
[83]	EP	1550 nm	Micro-resonator	Erbium ion dopants	Nanoparticle	$\varepsilon^{1/2}$	High	Moderate
[88]	EP	~250 THz	Micro-resonator	–	Anti-immunoglobulin G	$\varepsilon^{1/2}$	Low	Moderate
[90]]	EP	~10 GHz	Optical gyroscope	Brillouin gain	Rotation of input wave	$\varepsilon^{1/2}$	Moderate	Moderate
[92]	EP	1550 nm	Micro-resonator	Optical beam	Refractive index	$\varepsilon^{1/4}$	Low	Moderate
[86]	EP	~200 MHz	Electronic oscillator	NIC	Pressure	$\varepsilon^{1/2}$	High	Moderate
[97]	EP	~1 MHz	Electronic oscillator	NIC	Microfluid/ pressure/ acceleration	$\varepsilon^{1/4}$	High	Low
[99]	EP	~3 MHz	Electronic oscillator	NIC	Acceleration	$\varepsilon^{1/2}$	High	Low
[104]	EP	~20 kHz	Acoustic loudspeaker	NIC	Acoustic power	–	Moderate	–
[107]	EP	~500 Hz	Elastic spring	Complex spring constant	Mass	$\varepsilon^{1/2}$	Low	–
[122]	CPAL	~2 THz	Metasurface	Active metasurface	Normalized perturbation	$\varepsilon^2/\delta x$	High	Low
[43]	CPAL	~15 MHz	Electronic oscillator	NIC	Resistive/reactive perturbation	$\varepsilon^2/\delta x$	Moderate	Low
[129]	CPAL	~200 MHz	Electronic oscillator	Simulation	Resistive/reactive perturbation	–	Moderate	–
[130]	CPAL	~120 Hz	Thin elastic plate	NIC and piezoelectric media	Small vibration	–	–	Low
[131]	CPAL	~4000 Hz	Sandwich structure of acoustic materials	Complex mass density	Air pressure	–	–	Low

"–" represents that the reference does not provide a numerical or analytical demonstration for this evaluation; "δx" is a measure of fabrication error introduced into the system.

proved by adopting the complementary metal-semiconductor oxide (CMOS) technology to manufacture the sensor, such that parasitic effects can be eliminated, bringing the operating point closer to the self-dual singular point. Recently, a research group at Zhejiang University proposed a frequency-tunable CPAL-based electronic sensor [129]. The sensor is based on the same circuit topology in Fig. 9(b), but exploits a different sensing protocol. The authors reported that by introducing resistive, capacitive, or inductive perturbations in parallel with the CPAL structure, the CPAL frequency can be substantially shifted especially under reactive perturbations [see Fig. 9(b)]. The output factor is more likely to be affected by resistive perturbations [see Fig. 9(b)]. This paper shows that the sensing mechanism of the CPAL sensor may not be limited to the monochromatic setup, but can also be extended to the observation of CPAL frequency offset, even though the impact of phase/flicker noise is still uncertain. In [130], the CPAL effect was observed using a PT-symmetric thin elastic plate (TEP) shown in Fig. 9(c). In this case, gain and loss are realized by properly engineering the imaginary parts of Young's modulus of the TEP; for example, gain can be achieved with a piezoelectric TEP loaded with an NIC. This work also demonstrates that the elastic CPAL device can be used to detect vibrational perturbations with ultrahigh sensitivity. In [131], an acoustic CPAL sensor was proposed for air pressure sensing, as illustrated in Fig. 9(d). This PT-symmetric acoustic system consists of media with complex conjugated densities and an air cavity. By adjusting the thickness of the active and passive blocks, the sys-

tem can exhibit the CPAL effect at 4 kHz. Moreover, the CPAL frequency shift due to air pressure applied to the incompressible medium can be quite sensitive, with sensitivity in the order of 10^4 Hz per unit mass density. Table 1 summarizes the performance, pros and cons of EP-based and CPAL-based sensors discussed above [132–139]. In general, high entropy near an EP may cause the EP-based sensors to suffer from flicker/phase noise, which in turn degrade the signal-to-noise ratio and the reliability of sensor. Although the monochromatic CPAL-based sensors are immune to flicker/phase noise, the design challenge lies in how to coherently tune the complex amplitude ratio between the two incident waves, which requires precise control of amplitude and phase by using advanced attenuators and phase shifters. Nonetheless, both sensing mechanisms can detect small-scale perturbations, with much enhanced sensitivity compared to conventional DP-based and Hermitian sensors. Finally, we note that EPs and the associated bifurcation effect also exist in other non-Hermitian wave systems beyond PT-symmetry such as some time-modulated passive structures. However, in order to achieve the CPAL effect, gain and active component are indispensable, which should also be taken into consideration in the sensor design.

4. CONCLUSIONS

PT symmetry, originally discovered in non-Hermitian quantum mechanics, has now spawned many interesting applications in versatile wave systems and over a wide range of wavelengths. Among them, PT-symmetric sensors with enhanced sensitivity through EP and CPAL singularities have been extensively studied and emerged as one of the most promising applications of PT-symmetry and non-Hermitian physics. This review article provides an overview of both EP- and CPAL-based sensors in the realms of electromagnetics, optics, electronics, and acoustics. In general, EP-based sensors can leverage the bifurcation effect in the proximity of an EP to achieve unprecedentedly high sensitivity in terms of resonance frequency shift in response to small perturbations. On the other hand, in CPAL devices, the large modulation depth between the lasing mode and CPA mode can be exploited to make an ultrasensitive monochromatic sensor whose output factor at the CPAL frequency is susceptible to perturbations. Here, we have reported on principles of operation, opportunities, and challenges in the rapidly growing field of PT-symmetric sensors, which paves a promising path for the next-generation physical, chemical, biomedical, industrial, and environmental sensing devices and systems.

REFERENCES

[1] Rana, M. and V. Mittal, "Wearable sensors for real-time kinematics analysis in sports: A review," *IEEE Sensors Journal*, Vol. 21, No. 2, 1187–1207, Jan. 2021.

[2] Fleming, W. J., "New automotive sensors — A review," *IEEE Sensors Journal*, Vol. 8, No. 11, 1900–1921, Nov. 2008.

[3] Fleming, W. J., "Overview of automotive sensors," *IEEE Sensors Journal*, Vol. 1, No. 4, 296–308, Dec. 2001.

[4] Nazemi, H., A. Joseph, J. Park, and A. Emadi, "Advanced micro-and nano-gas sensor technology: A review," *Sensors*, Vol. 19, No. 6, 1285, Mar. 2019.

[5] Majhi, S. M., A. Mirzaei, H. W. Kim, S. S. Kim, and T. W. Kim, "Recent advances in energy-saving chemiresistive gas sensors: A review," *Nano Energy*, Vol. 79, 105369, Jan. 2021.

[6] Yamazoe, N., "Toward innovations of gas sensor technology," *Sensors and Actuators B: Chemical*, Vol. 108, No. 1-2, 2–14, Jul. 2005.

[7] Parrilla, M., M. Cuartero, and G. A. Crespo, "Wearable potentiometric ion sensors," *TrAC Trends in Analytical Chemistry*, Vol. 110, 303–320, Jan. 2019.

[8] Zhang, Y.-N., Y. Sun, L. Cai, Y. Gao, and Y. Cai, "Optical fiber sensors for measurement of heavy metal ion concentration: A review," *Measurement*, Vol. 158, 107742, Jul. 2020.

[9] Gershenfeld, N., R. Krikorian, and D. Cohen, "The internet of things," *Scientific American*, Vol. 291, No. 4, 76–81, Oct. 2004.

[10] Holler, J., V. Tsiatsis, C. Mulligan, S. Karnouskos, S. Avesand, and D. Boyle, *Internet of Things*, Academic Press, 2014.

[11] Kocakulak, M. and I. Butun, "An overview of wireless sensor networks towards internet of things," in *2017 IEEE 7th Annual Computing and Communication Workshop and Conference (CCWC)*, Las Vegas, NV, USA, Jan. 2017.

[12] Khalil, N., M. R. Abid, D. Benhaddou, and M. Gerndt, "Wireless sensors networks for internet of things," in *2014 IEEE Ninth International Conference on Intelligent Sensors, Sensor Networks and Information Processing (ISSNIP)*, Singapore, Apr. 2014.

[13] Ko, J., C. Lu, M. B. Srivastava, J. A. Stankovic, A. Terzis, and M. Welsh, "Wireless sensor networks for healthcare," *Proceedings of the IEEE*, Vol. 98, No. 11, 1947–1960, Nov. 2010.

[14] Yao, S., P. Swetha, and Y. Zhu, "Nanomaterial-enabled wearable sensors for healthcare," *Advanced Healthcare Materials*, Vol. 7, No. 1, 1700889, Jan. 2018.

[15] Ye, Z., Y. Ling, M. Yang, Y. Xu, L. Zhu, Z. Yan, and P.-Y. Chen, "A breathable, reusable, and zero-power smart face mask for wireless cough and mask-wearing monitoring," *ACS Nano*, Vol. 16, No. 4, 5874–5884, Mar. 2022.

[16] Ho, C. K., A. Robinson, D. R. Miller, and M. J. Davis, "Overview of sensors and needs for environmental monitoring," *Sensors*, Vol. 5, No. 1, 4–37, 2005.

[17] Hanrahan, G., D. G. Patil, and J. Wang, "Electrochemical sensors for environmental monitoring: Design, development and applications," *Journal of Environmental Monitoring*, Vol. 6, No. 8, 657–664, 2004.

[18] Yang, M., Z. Ye, C.-H. Sun, L. Zhu, M. Hajizadegan, and P.-Y. Chen, "A lightweight, zero-power intermodulation sensor based on the graphene oscillator," *IEEE Sensors Journal*, Vol. 23, No. 3, 3243–3250, Feb. 2023.

[19] Wang, Z., J. Zhan, C. Duan, X. Guan, P. Lu, and K. Yang, "A review of vehicle detection techniques for intelligent vehicles," *IEEE Transactions on Neural Networks and Learning Systems*, Vol. 34, No. 8, 3811–3831, Aug. 2023.

[20] Li, L. and F.-Y. Wang, *Advanced Motion Control and Sensing for Intelligent Vehicles*, Springer Science & Business Media, 2007.

[21] Kuswandi, B., Y. Wicaksono, Jayus, A. Abdullah, L. Y. Heng, and M. Ahmad, "Smart packaging: Sensors for monitoring of food quality and safety," *Sensing and Instrumentation for Food Quality and Safety*, Vol. 5, 137–146, 2011.

[22] Loutfi, A., S. Coradeschi, G. K. Mani, P. Shankar, and J. B. B. Rayappan, "Electronic noses for food quality: A review," *Journal of Food Engineering*, Vol. 144, 103–111, Jan. 2015.

[23] Sun, H., C. Ye, G. Zhao, H. Zhang, Z. Liu, W. Dai, J. Wang, F. E. Alam, Q. Yan, X. Li, J. Xu, C.-Y. Chen, P. Zhao, J. Ye,

N. Jiang, D. Chen, S. Wu, J. Kong, and C.-T. Lin, "Ultrasensitive micro/nanocrack-based graphene nanowall strain sensors derived from the substrate's Poisson's ratio effect," *Journal of Materials Chemistry A*, Vol. 8, No. 20, 10 310–10 317, May 2020.

[24] Jung, J., K. K. Kim, Y. D. Suh, S. Hong, J. Yeo, and S. H. Ko, "Recent progress in controlled nano/micro cracking as an alternative nano-patterning method for functional applications," *Nanoscale Horizons*, Vol. 5, No. 7, 1036–1049, Jul. 2020.

[25] Cao, W., Q. Liu, and Z. He, "Review of pavement defect detection methods," *IEEE Access*, Vol. 8, 14 531–14 544, 2020.

[26] Kerski, J., P. Lochner, A. Ludwig, A. D. Wieck, A. Kurzmann, A. Lorke, and M. Geller, "Quantum sensor for nanoscale defect characterization," *Physical Review Applied*, Vol. 15, No. 2, 024029, Feb. 2021.

[27] Burns, A., P. Sengupta, T. Zedayko, B. Baird, and U. Wiesner, "Core/shell fluorescent silica nanoparticles for chemical sensing: Towards single-particle laboratories," *Small*, Vol. 2, No. 6, 723–726, 2006.

[28] Wiersig, J., "Distance between exceptional points and diabolic points and its implication for the response strength of non-Hermitian systems," *Physical Review Research*, Vol. 4, No. 3, 033179, Sep. 2022.

[29] Berry, M. V. and M. Wilkinson, "Diabolical points in the spectra of triangles," *Proceedings of the Royal Society of London. Series A*, Vol. 392, No. 1802, 15–43, 1984.

[30] Ashida, Y., Z. Gong, and M. Ueda, "Non-hermitian physics," *Advances in Physics*, Vol. 69, No. 3, 249–435, 2020.

[31] Moiseyev, N., *Non-Hermitian Quantum Mechanics*, Cambridge University Press, 2011.

[32] Bender, C. M., "Making sense of non-hermitian hamiltonians," *Reports on Progress in Physics*, Vol. 70, No. 6, 947, 2007.

[33] Bender, C. M., S. Boettcher, and P. N. Meisinger, "PT-symmetric quantum mechanics," *Journal of Mathematical Physics*, Vol. 40, No. 5, 2201–2229, 1999.

[34] El-Ganainy, R., K. G. Makris, M. Khajavikhan, Z. H. Musslimani, S. Rotter, and D. N. Christodoulides, "Non-Hermitian physics and PT symmetry," *Nature Physics*, Vol. 14, No. 1, 11–19, 2018.

[35] Schindler, J., Z. Lin, J. M. Lee, H. Ramezani, F. M. Ellis, and T. Kottos, "PT-symmetric electronics," *Journal of Physics A: Mathematical and Theoretical*, Vol. 45, No. 44, 444029, 2012.

[36] Bender, C. M. and S. Boettcher, "Real spectra in non-Hermitian Hamiltonians having PT symmetry," *Physical Review Letters*, Vol. 80, No. 24, 5243, 1998.

[37] Bender, C. M., M. V. Berry, and A. Mandilara, "Generalized PT symmetry and real spectra," *Journal of Physics A: Mathematical and General*, Vol. 35, No. 31, L467, 2002.

[38] Heiss, W. D., "Exceptional points of non-hermitian operators," *Journal of Physics A: Mathematical and General*, Vol. 37, No. 6, 2455–2464, 2004.

[39] Stehmann, T., W. D. Heiss, and F. G. Scholtz, "Observation of exceptional points in electronic circuits," *Journal of Physics A: Mathematical and General*, Vol. 37, No. 31, 7813, 2004.

[40] Rüter, C. E., K. G. Makris, R. El-Ganainy, D. N. Christodoulides, M. Segev, and D. Kip, "Observation of parity-time symmetry in optics," *Nature Physics*, Vol. 6, No. 3, 192–195, 2010.

[41] Longhi, S., "PT-symmetric laser absorber," *Physical Review A*, Vol. 82, No. 3, 031801, Sep. 2010.

[42] Wong, Z. J., Y.-L. Xu, J. Kim, K. O'Brien, Y. Wang, L. Feng, and X. Zhang, "Lasing and anti-lasing in a single cavity," *Nature Photonics*, Vol. 10, No. 12, 796–801, Dec. 2016.

[43] Yang, M., Z. Ye, M. Farhat, and P.-Y. Chen, "Enhanced radio-frequency sensors based on a self-dual emitter-absorber," *Physical Review Applied*, Vol. 15, No. 1, 014026, Jan. 2021.

[44] Dembowski, C., B. Dietz, H. D. Gräf, H. L. Harney, A. Heine, W. D. Heiss, and A. Richter, "Encircling an exceptional point," *Physical Review E*, Vol. 69, No. 5, 056216, May 2004.

[45] Miri, M.-A. and A. Alù, "Exceptional points in optics and photonics," *Science*, Vol. 363, No. 6422, eaar7709, Jan. 2019.

[46] Heiss, W. D., "The physics of exceptional points," *Journal of Physics A: Mathematical and Theoretical*, Vol. 45, No. 44, 444016, 2012.

[47] Özdemir, S. K., S. Rotter, F. Nori, and L. Yang, "Parity-time symmetry and exceptional points in photonics," *Nature Materials*, Vol. 18, No. 8, 783–798, 2019.

[48] Feng, L., Y.-L. Xu, W. S. Fegadolli, M.-H. Lu, J. E. B. Oliveira, V. R. Almeida, Y.-F. Chen, and A. Scherer, "Experimental demonstration of a unidirectional reflectionless parity-time metamaterial at optical frequencies," *Nature Materials*, Vol. 12, No. 2, 108–113, Feb. 2013.

[49] Huang, Y., Y. Shen, C. Min, S. Fan, and G. Veronis, "Unidirectional reflectionless light propagation at exceptional points," *Nanophotonics*, Vol. 6, No. 5, 977–996, Sep. 2017.

[50] Huang, Y., G. Veronis, and C. Min, "Unidirectional reflectionless propagation in plasmonic waveguide-cavity systems at exceptional points," *Optics Express*, Vol. 23, No. 23, 29 882–29 895, Nov. 2015.

[51] Zhang, B., N. Chen, H. Yang, Y. Chen, J. Dong, H. Zhou, X. Zhang, and J. Xu, "Dispersion-suppressed mode depletion by exceptional points for on-chip nonlinear optics," *Physical Review Applied*, Vol. 18, No. 3, 034028, Sep. 2022.

[52] Parto, M., Y. G. N. Liu, B. Bahari, M. Khajavikhan, and D. N. Christodoulides, "Non-hermitian and topological photonics: Optics at an exceptional point," *Nanophotonics*, Vol. 10, No. 1, 403–423, Jan. 2020.

[53] Suchkov, S. V., A. A. Sukhorukov, J. Huang, S. V. Dmitriev, C. Lee, and Y. S. Kivshar, "Nonlinear switching and solitons in PT-symmetric photonic systems," *Laser & Photonics Reviews*, Vol. 10, No. 2, 177–213, Mar. 2016.

[54] Zhao, H. and L. Feng, "Parity-time symmetric photonics," *National Science Review*, Vol. 5, No. 2, 183–199, Mar. 2018.

[55] Zyablovsky, A. A., A. P. Vinogradov, A. A. Pukhov, A. V. Dorofeenko, and A. A. Lisyansky, "PT-symmetry in optics," *Physics-Uspekhi*, Vol. 57, No. 11, 1063–1082, 2014.

[56] Zhong, Q., S. Nelson, S. K. Özdemir, and R. El-Ganainy, "Controlling directional absorption with chiral exceptional surfaces," *Optics Letters*, Vol. 44, No. 21, 5242–5245, Nov. 2019.

[57] Zhong, Q., A. Hashemi, S. K. Özdemir, and R. El-Ganainy, "Control of spontaneous emission dynamics in microcavities with chiral exceptional surfaces," *Physical Review Research*, Vol. 3, No. 1, 013220, Mar. 2021.

[58] Zhong, Q., J. Kou, S. K. Özdemir, and R. El-Ganainy, "Hierarchical construction of higher-order exceptional points," *Physical Review Letters*, Vol. 125, No. 20, 203602, Nov. 2020.

[59] Soleymani, S., Q. Zhong, M. Mokim, S. Rotter, R. El-Ganainy, and S. K. Ozdemir, "Chiral and degenerate perfect absorption on exceptional surfaces," *Nature Communications*, Vol. 13, No. 1, 599, Feb. 2022.

[60] Feng, L., Z. J. Wong, R.-M. Ma, Y. Wang, and X. Zhang, "Single-mode laser by parity-time symmetry breaking," *Science*, Vol. 346, No. 6212, 972–975, 2014.

[61] Yang, M., L. Zhu, Q. Zhong, R. El-Ganainy, and P.-Y. Chen, "Spectral sensitivity near exceptional points as a resource for hardware encryption," *Nature Communications*, Vol. 14, No. 1,

1145, Feb. 2023.

[62] Yang, M., Z. Ye, H. Pan, M. Farhat, A. E. Cetin, and P.-Y. Chen, "Electromagnetically unclonable functions generated by non-Hermitian absorber-emitter," *Science Advances*, Vol. 9, No. 36, Sep. 2023.

[63] Sakhdari, M., M. Hajizadegan, and P.-Y. Chen, "Robust extended-range wireless power transfer using a higher-order PT-symmetric platform," *Physical Review Research*, Vol. 2, No. 1, 013152, Feb. 2020.

[64] Hao, X., K. Yin, J. Zou, R. Wang, Y. Huang, X. Ma, and T. Dong, "Frequency-stable robust wireless power transfer based on high-order pseudo-hermitian physics," *Physical Review Letters*, Vol. 130, No. 7, 077202, Feb. 2023.

[65] Ye, Z., M. Yang, and P.-Y. Chen, "Multi-band parity-time-symmetric wireless power transfer systems for ISM-band bio-implantable applications," *IEEE Journal of Electromagnetics, RF and Microwaves in Medicine and Biology*, Vol. 6, No. 2, 196–203, Jun. 2022.

[66] Wei, Z. and B. Zhang, "Transmission range extension of PT-symmetry-based wireless power transfer system," *IEEE Transactions on Power Electronics*, Vol. 36, No. 10, 11 135–11 147, Oct. 2021.

[67] Assawaworrarit, S., X. Yu, and S. Fan, "Robust wireless power transfer using a nonlinear parity-time-symmetric circuit," *Nature*, Vol. 546, No. 7658, 387–390, Jun. 2017.

[68] Assawaworrarit, S. and S. Fan, "Robust and efficient wireless power transfer using a switch-mode implementation of a nonlinear parity-time symmetric circuit," *Nature Electronics*, Vol. 3, No. 5, 273–279, 2020.

[69] Slobodkin, Y., G. Weinberg, H. Hoerner, K. Pichler, S. Rotter, and O. Katz, "Massively degenerate coherent perfect absorber for arbitrary wavefronts," *Science*, Vol. 377, No. 6609, 995–998, Aug. 2022.

[70] Noh, H., Y. Chong, A. D. Stone, and H. Cao, "Perfect coupling of light to surface plasmons by coherent absorption," *Physical Review Letters*, Vol. 108, No. 18, 186805, May 2012.

[71] Chong, Y. D. and A. D. Stone, "Hidden black: Coherent enhancement of absorption in strongly scattering media," *Physical Review Letters*, Vol. 107, No. 16, 163901, Oct. 2011.

[72] Chong, Y. D., L. Ge, H. Cao, and A. D. Stone, "Coherent perfect absorbers: Time-reversed lasers," *Physical Review Letters*, Vol. 105, No. 5, 053901, Jul. 2010.

[73] Bai, P., K. Ding, G. Wang, J. Luo, Z.-Q. Zhang, C. T. Chan, Y. Wu, and Y. Lai, "Simultaneous realization of a coherent perfect absorber and laser by zero-index media with both gain and loss," *Physical Review A*, Vol. 94, No. 6, 063841, Dec. 2016.

[74] Sakhdari, M., N. M. Estakhri, H. Bagci, and P.-Y. Chen, "Low-threshold lasing and coherent perfect absorption in generalized PT-symmetric optical structures," *Physical Review Applied*, Vol. 10, No. 2, 024030, 2018.

[75] Ha, T. D., C.-H. Sun, M. Farhat, and P.-Y. Chen, "Reconfigurable superdirective beamshaping using a PTX-synthesis metasurface," *Optical Materials Express*, Vol. 13, No. 3, 646–655, Mar. 2023.

[76] Hajizadegan, M., L. Zhu, and P.-Y. Chen, "Superdirective leaky radiation from a PT-synthetic metachannel," *Optics Express*, Vol. 29, No. 8, 12 330–12 343, Apr. 2021.

[77] Fu, Y.-Y., Y. Fei, D.-X. Dong, and Y.-W. Liu, "Photonic spin Hall effect in PT symmetric metamaterials," *Frontiers of Physics*, Vol. 14, No. 6, 62601, 2019.

[78] Liu, T., X. Zhu, F. Chen, S. Liang, and J. Zhu, "Unidirectional wave vector manipulation in two-dimensional space with an all passive acoustic parity-time-symmetric metamaterials crystal," *Physical Review Letters*, Vol. 120, No. 12, 124502, Mar. 2018.

[79] Zhang, X.-L., T. Jiang, and C. T. Chan, "Dynamically encircling an exceptional point in anti-parity-time symmetric systems: Asymmetric mode switching for symmetry-broken modes," *Light: Science & Applications*, Vol. 8, No. 1, 88, Oct. 2019.

[80] Chen, P.-Y. and R. El-Ganainy, "Exceptional points enhance wireless readout," *Nature Electronics*, Vol. 2, No. 8, 323–324, Aug. 2019.

[81] Mortensen, N. A., P. A. D. Gonçalves, M. Khajavikhan, D. N. Christodoulides, C. Tserkezis, and C. Wolff, "Fluctuations and noise-limited sensing near the exceptional point of parity-time-symmetric resonator systems," *Optica*, Vol. 5, No. 10, 1342–1346, Oct. 2018.

[82] Haus, H. A. and W. Huang, "Coupled-mode theory," *Proceedings of the IEEE*, Vol. 79, No. 10, 1505–1518, Oct. 1991.

[83] Chen, W., S. K. Özdemir, G. Zhao, J. Wiersig, and L. Yang, "Exceptional points enhance sensing in an optical microcavity," *Nature*, Vol. 548, No. 7666, 192–196, Aug. 2017.

[84] Schindler, J., A. Li, M. C. Zheng, F. M. Ellis, and T. Kottos, "Experimental study of active LRC circuits with PT symmetries," *Physical Review A*, Vol. 84, No. 4, 040101, Oct. 2011.

[85] Sakhdari, M., M. Hajizadegan, Y. Li, M. M.-C. Cheng, J. C. H. Hung, and P.-Y. Chen, "Ultrasensitive, parity-time-symmetric wireless reactive and resistive sensors," *IEEE Sensors Journal*, Vol. 18, No. 23, 9548–9555, Dec. 2018.

[86] Chen, P.-Y., M. Sakhdari, M. Hajizadegan, Q. Cui, M. M.-C. Cheng, R. El-Ganainy, and A. Alu, "Generalized parity-time symmetry condition for enhanced sensor telemetry," *Nature Electronics*, Vol. 1, No. 5, 297–304, May 2018.

[87] Yang, M., Z. Ye, and P.-Y. Chen, "A quantum-inspired biotelemetry system for robust and ultrasensitive wireless intracranial pressure monitoring," in *2021 IEEE Sensors*, Sydney, Australia, Oct. 2021.

[88] Park, J.-H., A. Ndao, W. Cai, L. Hsu, A. Kodigala, T. Lepetit, Y.-H. Lo, and B. Kante, "Symmetry-breaking-induced plasmonic exceptional points and nanoscale sensing," *Nature Physics*, Vol. 16, No. 4, 462–468, 2020.

[89] Young, A. T., "Rayleigh-scattering," *Physics Today*, Vol. 35, No. 1, 42–48, 1982.

[90] Lai, Y.-H., Y.-K. Lu, M.-G. Suh, Z. Yuan, and K. Vahala, "Observation of the exceptional-point-enhanced sagnac effect," *Nature*, Vol. 576, No. 7785, 65–69, Dec. 2019.

[91] Post, E. J., "Sagnac effect," *Reviews of Modern Physics*, Vol. 39, No. 2, 475, 1967.

[92] Wu, Y., P. Zhou, T. Li, W. Wan, and Y. Zou, "High-order exceptional point based optical sensor," *Optics Express*, Vol. 29, No. 4, 6080–6091, Feb. 2021.

[93] Langbein, W., "No exceptional precision of exceptional-point sensors," *Physical Review A*, Vol. 98, No. 2, 023805, Aug. 2018.

[94] Chen, C., L. Jin, and R.-B. Liu, "Sensitivity of parameter estimation near the exceptional point of a non-hermitian system," *New Journal of Physics*, Vol. 21, No. 8, 083002, Aug. 2019.

[95] Duggan, R., S. A. Mann, and A. Alù, "Limitations of sensing at an exceptional point," *ACS Photonics*, Vol. 9, No. 5, 1554–1566, 2022.

[96] Hodaei, H., A. U. Hassan, S. Wittek, H. Garcia-Gracia, R. El-Ganainy, D. N. Christodoulides, and M. Khajavikhan, "Enhanced sensitivity at higher-order exceptional points," *Nature*, Vol. 548, No. 7666, 187–191, Aug. 2017.

[97] Xiao, Z., H. Li, T. Kottos, and A. Alu, "Enhanced sensing and nondegraded thermal noise performance based on PT-

symmetric electronic circuits with a sixth-order exceptional point," *Physical Review Letters*, Vol. 123, No. 21, 213901, Nov. 2019.

[98] Geng, Q. and K.-D. Zhu, "Discrepancy between transmission spectrum splitting and eigenvalue splitting: A reexamination on exceptional point-based sensors," *Photonics Research*, Vol. 9, No. 8, 1645–1649, Aug. 2021.

[99] Kononchuk, R., J. Cai, F. Ellis, R. Thevamaran, and T. Kottos, "Exceptional-point-based accelerometers with enhanced signal-to-noise ratio," *Nature*, Vol. 607, No. 7920, 697–702, Jul. 2022.

[100] Zhu, X., H. Ramezani, C. Shi, J. Zhu, and X. Zhang, "PT-symmetric acoustics," *Physical Review X*, Vol. 4, No. 3, 031042, Sep. 2014.

[101] Shi, C., M. Dubois, Y. Chen, L. Cheng, H. Ramezani, Y. Wang, and X. Zhang, "Accessing the exceptional points of parity-time symmetric acoustics," *Nature Communications*, Vol. 7, No. 1, 11110, Mar. 2016.

[102] Shen, C., J. Li, X. Peng, and S. A. Cummer, "Synthetic exceptional points and unidirectional zero reflection in non-Hermitian acoustic systems," *Physical Review Materials*, Vol. 2, No. 12, 125203, Dec. 2018.

[103] Fang, X., N. J. R. K. Gerard, Z. Zhou, H. Ding, N. Wang, B. Jia, Y. Deng, X. Wang, Y. Jing, and Y. Li, "Observation of higher-order exceptional points in a non-local acoustic metagrating," *Communications Physics*, Vol. 4, No. 1, 271, Dec. 2021.

[104] Fleury, R., D. Sounas, and A. Alù, "An invisible acoustic sensor based on parity-time symmetry," *Nature Communications*, Vol. 6, No. 1, 5905, Jan. 2015.

[105] Ge, L., Y. D. Chong, and A. D. Stone, "Conservation relations and anisotropic transmission resonances in one-dimensional PT-symmetric photonic heterostructures," *Physical Review A*, Vol. 85, No. 2, 023802, Feb. 2012.

[106] Wang, C., W. R. Sweeney, A. D. Stone, and L. Yang, "Coherent perfect absorption at an exceptional point," *Science*, Vol. 373, No. 6560, 1261–1265, Sep. 2021.

[107] Rosa, M. I. N., M. Mazzotti, and M. Ruzzene, "Exceptional points and enhanced sensitivity in PT-symmetric continuous elastic media," *Journal of the Mechanics and Physics of Solids*, Vol. 149, 104325, Apr. 2021.

[108] Chen, W., J. Zhang, B. Peng, S. K. Özdemir, X. Fan, and L. Yang, "Parity-time-symmetric whispering-gallery mode nanoparticle sensor [invited]," *Photonics Research*, Vol. 6, No. 5, A23–A30, May 2018.

[109] Zaky, Z. A., M. Al-Dossari, A. Sharma, and A. H. Aly, "Effective pressure sensor using the parity-time symmetric photonic crystal," *Physica Scripta*, Vol. 98, No. 3, 035522, 2023.

[110] Zhong, Q., J. Ren, M. Khajavikhan, D. N. Christodoulides, S. K. Özdemir, and R. El-Ganainy, "Sensing with exceptional surfaces in order to combine sensitivity with robustness," *Physical Review Letters*, Vol. 122, No. 15, 153902, Apr. 2019.

[111] Djorwe, P., Y. Pennec, and B. Djafari-Rouhani, "Exceptional point enhances sensitivity of optomechanical mass sensors," *Physical Review Applied*, Vol. 12, No. 2, 024002, Aug. 2019.

[112] Chen, P.-Y. and J. Jung, "PT symmetry and singularity-enhanced sensing based on photoexcited graphene metasurfaces," *Physical Review Applied*, Vol. 5, No. 6, 064018, Jun. 2016.

[113] Zhou, B.-B., W.-J. Deng, L.-F. Wang, L. Dong, and Q.-A. Huang, "Enhancing the remote distance of LC passive wireless sensors by parity-time symmetry breaking," *Physical Review Applied*, Vol. 13, No. 6, 064022, Jun. 2020.

[114] Yin, K., Y. Huang, C. Ma, X. Hao, X. Gao, X. Ma, and T. Dong, "Wireless real-time capacitance readout based on perturbed nonlinear parity-time symmetry," *Applied Physics Letters*, Vol. 120, No. 19, 194101, 2022.

[115] Sakhdari, M., M. Hajizadegan, Q. Zhong, D. N. Christodoulides, R. El-Ganainy, and P.-Y. Chen, "Experimental observation of PT symmetry breaking near divergent exceptional points," *Physical Review Letters*, Vol. 123, No. 19, 193901, 2019.

[116] Ye, Z., M. Yang, N. Alsaab, and P.-Y. Chen, "A wireless, zero-power and multiplexed sensor for wound monitoring," in *2022 IEEE Sensors*, 1–4, Dallas, TX, USA, Oct. 2022.

[117] Sakhdari, M., Z. Ye, M. Farhat, and P.-Y. Chen, "Generalized theory of PT-symmetric radio-frequency systems with divergent exceptional points," *IEEE Transactions on Antennas and Propagation*, Vol. 70, No. 10, 9396–9405, 2022.

[118] Sakhdari, M. and P.-Y. Chen, "Ultrasensitive telemetric sensor based on adapted parity-time symmetry," in *2017 IEEE International Symposium on Antennas and Propagation & USNC/URSI National Radio Science Meeting*, 579–580, San Diego, CA, USA, Jul. 2017.

[119] Fleury, R., D. L. Sounas, and A. Alù, "Parity-time symmetry in acoustics: Theory, devices, and potential applications," *IEEE Journal of Selected Topics in Quantum Electronics*, Vol. 22, No. 5, 121–129, 2016.

[120] Igoshin, V., M. Tsimokha, A. Nikitina, M. Petrov, I. Toftul, and K. Frizyuk, "Exceptional points in single open acoustic resonator due to the symmetry breaking," *Arxiv Preprint Arxiv:2305.02370*, 2023.

[121] Pozar, D. M., *Microwave Engineering*, 4th ed., Hoboken, NJ : Wiley, 2012.

[122] Farhat, M., M. Yang, Z. Ye, and P.-Y. Chen, "PT-symmetric absorber-laser enables electromagnetic sensors with unprecedented sensitivity," *ACS Photonics*, Vol. 7, No. 8, 2080–2088, 2020.

[123] Ye, Z., M. Farhat, and P.-Y. Chen, "Tunability and switching of Fano and Lorentz resonances in PTX-symmetric electronic systems," *Applied Physics Letters*, Vol. 117, No. 3, 031101, 2020.

[124] Yang, M., Z. Ye, M. Farhat, and P.-Y. Chen, "Cascaded PT-symmetric artificial sheets: Multimodal manipulation of self-dual emitter-absorber singularities, and unidirectional and bidirectional reflectionless transparencies," *Journal of Physics D: Applied Physics*, Vol. 55, No. 8, 085301, 2021.

[125] Watanabe, T., T. Fukushima, Y. Yabe, S. A. B. Tombet, A. Satou, A. A. Dubinov, V. Y. Aleshkin, V. Mitin, V. Ryzhii, and T. Otsuji, "The gain enhancement effect of surface plasmon polaritons on terahertz stimulated emission in optically pumped monolayer graphene," *New Journal of Physics*, Vol. 15, No. 7, 075003, 2013.

[126] Low, T., P.-Y. Chen, and D. N. Basov, "Superluminal plasmons with resonant gain in population inverted bilayer graphene," *Physical Review B*, Vol. 98, No. 4, 041403, 2018.

[127] Ye, Z., M. Yang, L. Zhu, and P.-Y. Chen, "PTX-symmetric metasurfaces for sensing applications," *Frontiers of Optoelectronics*, Vol. 14, 211–220, 2021.

[128] Lin, Z., H. Ramezani, T. Eichelkraut, T. Kottos, H. Cao, and D. N. Christodoulides, "Unidirectional invisibility induced by PT-symmetric periodic structures," *Physical Review Letters*, Vol. 106, No. 21, 213901, 2011.

[129] Wu, J., J. Li, C. Zhang, Y. Liu, L. Xu, W. Xuan, H. Jin, S. Dong, and J. Luo, "Frequency tunable coherent perfect absorption and lasing in radio-frequency system for ultrahigh-sensitive sensing," *Applied Physics Letters*, Vol. 123, No. 16, 164102, 2023.

[130] Farhat, M., P.-Y. Chen, S. Guenneau, and Y. Wu, "Self-dual singularity through lasing and antilasing in thin elastic plates," *Physical Review B*, Vol. 103, No. 13, 134101, 2021.

[131] Farhat, M., W. W. Ahmad, A. Khelif, K. N. Salama, and Y. Wu, "Enhanced acoustic pressure sensors based on coherent perfect absorber-laser effect," *Journal of Applied Physics*, Vol. 129, No. 10, 104902, 2021.

[132] Dong, Z., Z. Li, F. Yang, C.-W. Qiu, and J. S. Ho, "Sensitive readout of implantable microsensors using a wireless system locked to an exceptional point," *Nature Electronics*, Vol. 2, No. 8, 335–342, 2019.

[133] Chen, L. Y., B. C.-K. Tee, A. L. Chortos, G. Schwartz, V. Tse, D. J. Lipomi, H.-S. P. Wong, M. V. McConnell, and Z. Bao, "Continuous wireless pressure monitoring and mapping with ultra-small passive sensors for health monitoring and critical care," *Nature Communications*, Vol. 5, No. 1, 5028, 2014.

[134] Yang, M., Z. Ye, M. Farhat, and P.-Y. Chen, "Ultrarobust wireless interrogation for sensors and transducers: A non-hermitian telemetry technique," *IEEE Transactions on Instrumentation and Measurement*, Vol. 70, 1–9, 2021.

[135] Yang, M., Z. Ye, N. Alsaab, M. Farhat, and P.-Y. Chen, "In-vitro demonstration of ultra-reliable, wireless and batteryless implanted intracranial sensors operated on loci of exceptional points," *IEEE Transactions on Biomedical Circuits and Systems*, Vol. 16, No. 2, 287–295, 2022.

[136] Hajizadegan, M., M. Sakhdari, S. Liao, and P.-Y. Chen, "High-sensitivity wireless displacement sensing enabled by PT-symmetric telemetry," *IEEE Transactions on Antennas and Propagation*, Vol. 67, No. 5, 3445–3449, 2019.

[137] Sakhdari, M., M. Farhat, and P.-Y. Chen, "PT-symmetric metasurfaces: wave manipulation and sensing using singular points," *New Journal of Physics*, Vol. 19, No. 6, 065002, 2017.

[138] Zhang, Y. J., H. Kwon, M.-A. Miri, E. Kallos, H. Cano-Garcia, M. S. Tong, and A. Alu, "Noninvasive glucose sensor based on parity-time symmetry," *Physical Review Applied*, Vol. 11, No. 4, 044049, 2019.

[139] Yang, M.-Y., Z.-L. Ye, L. Zhu, M. Farhat, and P.-Y. Chen, "Recent advances in coherent perfect absorber-lasers and their future applications," *Journal of Central South University*, Vol. 29, No. 10, 3203–3216, 2022.